Excited State Charge Separation in an Azobenzene-Bridged Perylenediimide Dimer – Effect of Photochemical Trans-Cis Isomerization

Nathalie Zink-Lorre[+],[a] Sairaman Seetharaman[+],[b] David Gutiérrez-Moreno,[a] Fernando Fernández-Lázaro,*[a] Paul A. Karr,[c] and Francis D'Souza*[b]

Dedicated to Professor Tomás Torres on the occasion of his 70th birthday.

Abstract: Photoinduced charge transfer and separation events in a newly synthesized azobenzene-bridged perylene-diimide-dimer (PDI-dimer) are demonstrated. Trans-to-cis conversion (~50% efficiency) from the initial trans PDI-dimer by 355 nm pulsed laser light, and its reversal, cis-to-trans, process by 435 nm laser light irradiation has been possible to accomplish. Efficient fluorescence quenching in the PDI-dimer, more so for the cis isomer was witnessed, and such quenching increased with increasing solvent polarity. DFT-calculated geometry and electronic structures helped in visualizing the charge transfer in the PDI-dimer in both isomeric forms, and also revealed certain degree of partic-ipation of the azobenzene entity in the charge transfer events. Femtosecond transient absorption spectral studies confirmed occurrence of both charge transfer followed by charge separation in the studied PDI-dimer in both trans and cis forms in polar solvents, and the evaluated time constants from Global target analysis revealed accelerated events in the cis PDI-dimer due to proximity effects. The present study offers key insights on the role of the azobenzene bridge, and the dimer geometry in governing the excited state charge transfer and separation in symmetrically linked PDI dimer.

Introduction

Symmetry breaking charge transfer (SBCT) occurs when a photoexcited molecule (S_1^*) is electronically coupled to an identical neighboring molecule in the ground state (S_o).[1] This excited state complex subsequently could undergo symmetry breaking charge separation (SBCS) wherein one molecule is oxidized and the other one is reduced, thus breaking charge-neutral symmetry to produce a radical ion-pair. This process has been utilized by nature in photosynthesis wherein excited chlorophyll dimer transfers the captured light energy to the reaction center via SBCS.[2] The process of SBCT and SBCS in intramolecular systems has been mainly studied in covalently linked dimers of perylenediimide, anthryl, phenalenyl, BODIPY, and polycyclic compounds both in solution and solid state.[1,3] This concept has been successfully utilized in various applica-tions including in artificial photosynthesis, and in building optoelectronic, photovoltaic and photonic devices.[1b,f]

The trans→cis isomerization of azobenzene, a diazene (HN≡NH) derivative, upon light irradiation of appropriate wave-length (in the 350 nm range) is well known (Figure 1a).[4] The reverse cis→trans isomerization can be driven by either light (irradiation in the 435 nm range) or thermally in the dark. Trans-azobenzene adopts a planar structure with C_{2h} symmetry while cis-azobenzene assumes a non-planar conformation with C_2 symmetry (~30° twist of the phenyl rings). The photochromic properties of azobenzene, including the remarkable photo-stability, have made it to be an ideal molecular entity for various molecular device applications, specifically as light triggered switches.[4,5]

A literature survey shows that although a change in cis-trans geometry upon isomerization orienting the molecule to perform specific task is known,[1,4,5] this concept has never been utilized to verify how this property would affect SBCT and SBCS when two identical fluorophores are connected to the azobenzene unit. With this in mind, in the present study, we have newly designed a perylenediimide dimer (see Figure 1b for structure) wherein the two PDI entities are symmetrically connected to an azobenzene spacer unit. As demonstrated

[a] Dr. N. Zink-Lorre,[+] Dr. D. Gutiérrez-Moreno, Prof. F. Fernández-Lázaro
Área de Química Orgánica, Instituto de Bioingeniería
Universidad Miguel Hernández de Elche
Avda. de la Universidad s/n, 03202 Elche (Spain)
E-mail: fdofdez@umh.es

[b] Dr. S. Seetharaman,[+] Prof. F. D'Souza
Department of Chemistry
University of North Texas
1155 Union Circle, #305070, Denton, TX 76203-5017 (USA)
E-mail: Francis.DSouza@UNT.edu

[c] Prof. P. A. Karr
Department of Physical Sciences and Mathematics
Wayne State College, 1111 Main Street, Wayne, Nebraska 68787 (USA)

[+] These authors contributed equally to this manuscript.

Chemistry–A European Journal

Full Paper
doi.org/10.1002/chem.202102903

Chemistry Europe
European Chemical
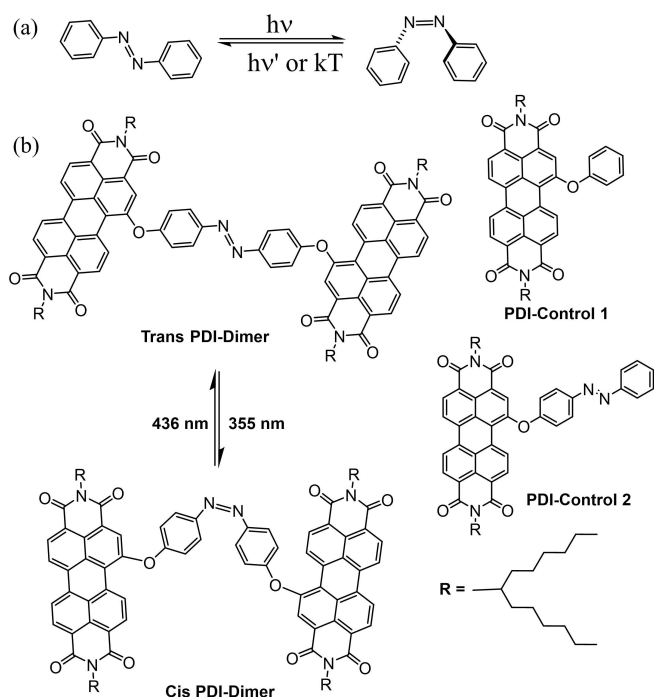Societies Publishing

Figure 1. (a) Isomerization of azobenzene entity. (b) Structure of the PDI-dimer in the photochemically produced trans and cis forms. PDI-control 1 and PDI-control 2 are the control compounds used in the present study.
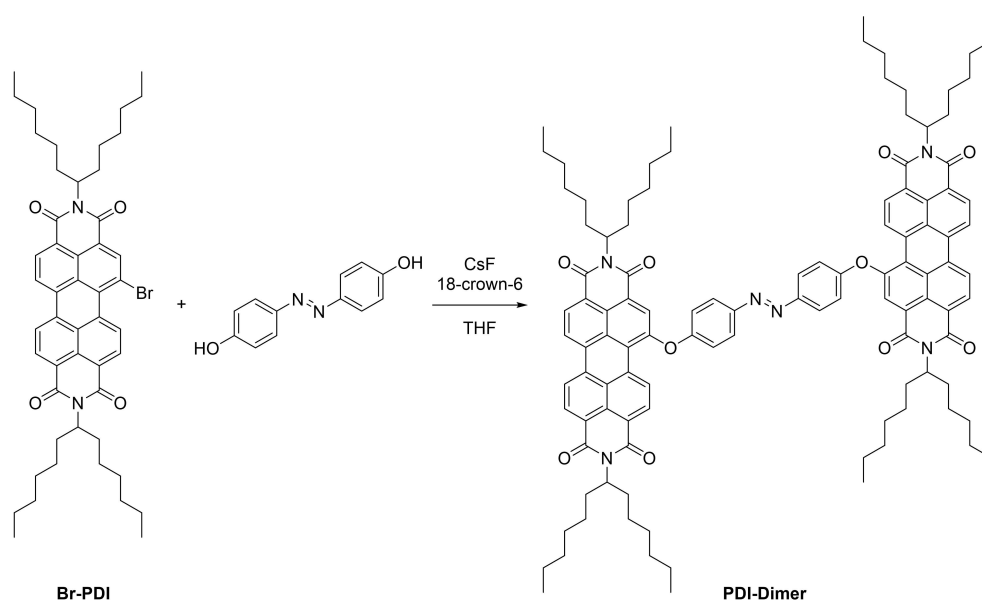
here, excited state charge transfer indeed occurs at an ultrafast time scale in the trans PDI-dimer wherein the spacer azobenzene contributes to this phenomenon. Interestingly, due to associated geometry changes, such a charge transfer process occurs even faster in the photochemically generated cis PDI-dimer. Additionally, in polar solvents, the charge transfer

product is further stabilized to yield charge separation product, PDI[•+]–PDI[•−]. The present azobenzene linked PDI-dimer demonstrates the significance of cis-trans isomerization in governing charge transfer and charge separation processes in symmetric dimers.

Results and Discussion

PDI-dimer was synthesized for the first time according to Scheme 1 by a fluoride-assisted nucleophilic substitution on a halogenated PDI, a procedure previously developed by us.[6] Thus, reaction of 1-bromoPDI[7] with 4,4'-dihydroxyazobenzene[8] in the presence of caesium fluoride and 18-crown-6 afforded the azo-bridged dimer in 46% yield. PDI-control 1 and PDI-control 2 were prepared using the same methodology. The synthetic details and the NMR and mass spectral data of all new three compounds are given in the Supporting Information (see Figures S1–S9 in Supporting Information). The ^{1}H NMR spectral data of PDI-Dimer were consistent with the trans isomer of the dimer.

The normalized absorption and fluorescence spectra of trans PDI-dimer are shown in Figure 2a. The PDI peaks were located at 498 and 532 nm, and revealed about 2 nm red-shift going from toluene (dielectric constant, $\varepsilon = 2.38$) to N,N-dimethylformamide (DMF, $\varepsilon = 37.7$). These spectral features were typical of PDI monomer[9] without any spectral broadening suggesting lack of ground state interactions between the PDI entities of the dimer.[10] Another broad peak at ~350 nm range was observed and was attributed to the azobenzene entity. It may be mentioned here that when compared to pure azobenzene (λ_{max} ~320 nm),[4c] the absorption maximum of this moiety in the PDI-dimer was found to be red-shifted by nearly 30 nm. This has been attributed to the electronic effects caused

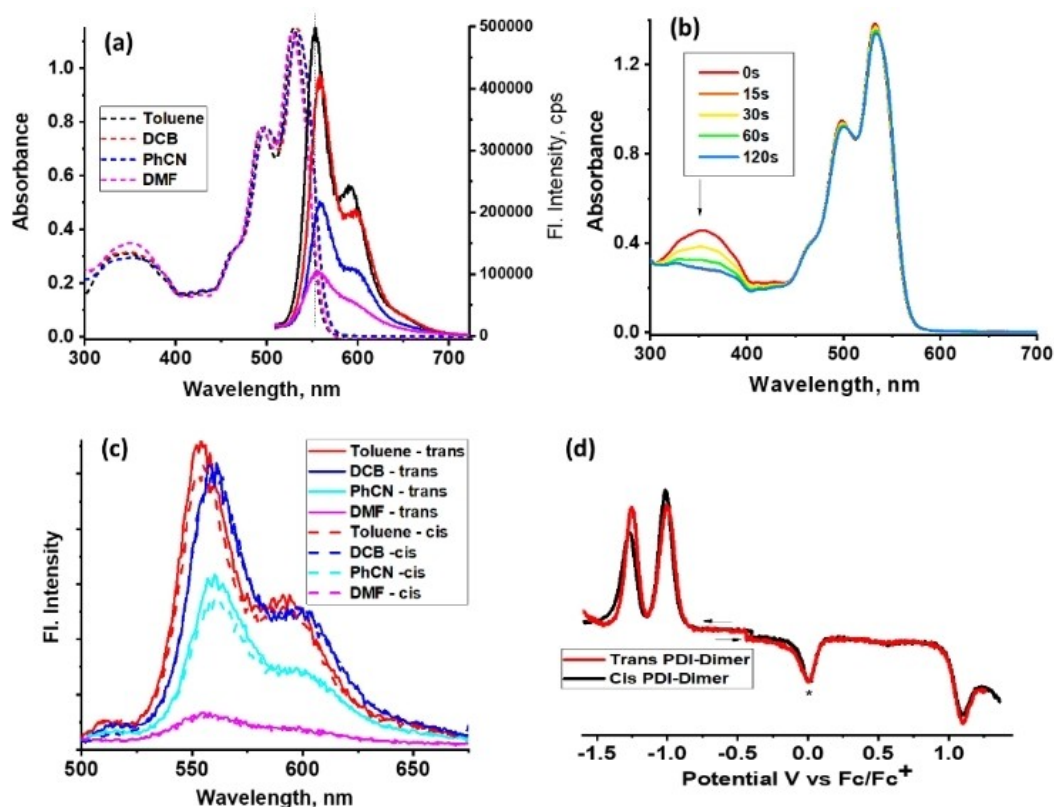**Scheme 1.** Synthesis of azobenzene bridged PDI-dimer.

Chemistry–A European Journal

Full Paper
doi.org/10.1002/chem.202102903

Chemistry
Europe
European Chemical
Societies Publishing

Figure 2. (a) Normalized absorption (dashed) and fluorescence spectra (solid lines, $\lambda_{ex} = 500$ nm) of trans PDI-dimer in toluene (black), DCB (red), PhCN (blue) and DMF (magenta). (b) Spectral changes associated with trans→cis/trans isomerization of PDI-dimer upon 355 nm pulsed laser irradiation (15 s each interval). (c) Comparative fluorescence spectra of trans (solid) and cis/trans (dashed) PDI-dimer in the indicated solvents. (d) Differential pulse voltammograms of trans (red) and cis/trans (black) PDI-dimer in benzonitrile containing 0.1 M (TBA)ClO$_4$. The '*' indicates oxidation peak of ferrocene used as an internal standard.

by the ether groups on the phenyl rings of azobenzene. This observation was also supported by the peak maxima of PDI-control 2, having only one phenoxy group on azobenzene, displaying the peak maximum at 335 nm (see Supporting Information, Figure S10). That is, systematic red-shift with increasing phenoxy groups on azobenzene entity was witnessed. Importantly, the sufficiently separated peak maxima of azobenzene and PDI entities in the PDI-dimer is notable for their selective excitation needed for observing successful photo-isomerization and subsequent charge transfer processes.

The fluorescence spectrum of PDI in the PDI-dimer revealed two peaks in the 555–592 nm range. The measured fluorescence quantum yields in CH$_2$Cl$_2$ were found to be 0.009 for PDI-Dimer, 0.4 for PDI-control 1, and 0.012 for PDI-control 2 with reference to pristine PDI ($\Phi_f = 1.0$). A decrease in the peak intensity with increasing solvent polarity was witnessed accompanied by a small red-shift of 4–5 nm (see Figure 2a). That is, going from less polar toluene to highly polar DMF a 80% quenching of fluorescence intensity was observed suggesting occurrence of excited state events in the trans PDI-dimer.[10] In order to ascertain this quenching is not as a consequence of simple solvent effect, emission of PDI-control 1 and -control 2 were also recorded in the investigated solvents (see Supporting Information–Figure S11). In both cases, the maximum quenching was less than 35% going from nonpolar toluene to polar

DMF. Noticeably, no spectral broadening of the PDI-dimer fluorescence peaks was observed suggesting lack of excimer formation in the excited state.[1f] From these data, the singlet excited state energy of PDI-dimer in solution, determined from the intersection of the absorption and fluorescence peaks, was found to be 2.27 eV.

Fluorescence lifetimes of PDI-controls and PDI-dimer in solvents of different polarity were also measured using time correlated single photon counting (TCSPC) technique, and the data are given in Table S1 (Supporting Information). PDI-control 1 revealed monoexponential decay with lifetimes ranging between 4.5 and 4.9 ns. Interestingly, the PDI-dimer and PDI-control 2 revealed biexponential decays with a major short-lived and a minor long-lived components both in polar and nonpolar solvents. The amplitude of the short-lived component increased with increasing solvent polarity. The lifetime of the short-lived component was within the time resolution of our TCSPC set up (~ 200 ps). Hence, more emphasis is given to femtosecond transient spectral data that will be discussed in subsequent sections.

Next, experiments to observe trans→cis isomerization were performed by irradiating the diazo entity, having an absorption maximum at 350 nm, in toluene using a pulsed laser set to this wavelength, as shown in Figure 2b. Similar observations were also made in other investigated solvents. During the course of

Chemistry–A European Journal

Full Paper
doi.org/10.1002/chem.202102903

Chemistry Europe
European Chemical
Societies Publishing

light irradiation, peak intensity of 350 nm decreased to reach a plateau without appreciable decrease in the intensity of the PDI peaks. The trans→cis isomerization was also probed by ^{1}H NMR studies (Figures S12 and S13 in Supporting Information). Figure S12 shows the aromatic zone of the ^{1}H NMR spectra of samples irradiated with an UV lamp at 365 nm for different lapses (from 1 to 10 minutes). Within the first minute of irradiation, it was possible to clearly observe the signal duplication corresponding to the cis-isomer formation. The integration of signals at 8.09 and 7.36 ppm, corresponding to the trans-azo moiety (see Figure S1, Supporting Information), decreases, while new signals at 7.23 and 7.10, attributed to the cis-isomer, appear. After 10 minutes of continuous irradiation about 1:1 mixture of trans and cis isomers was obtained. From these it was safe to conclude that the compound generated by photo-irradiation is approximately a 50:50 mixture of cis and trans isomers, and hence a cis/trans PDI-dimer nomenclature is used for the photo-irradiated PDI-dimer throughout this study.

At the end, the fluorescence spectrum of the cis/trans PDI-dimer was recorded in a given solvent and compared with the intensity of that of the trans-isomer as shown in Figure 2c. Irrespective of the solvent system, the shape of the emission spectrum was that of the trans PDI-dimer, however, with a decreased intensity that further decreased with solvent polarity. These results collectively point out to an improved quenching in the cis/trans PDI-dimer over the pure trans one. To ascertain whether the trans→cis/trans isomerization is reversible, the cis/trans sample was excited using 436 nm laser light as shown in Supporting Information, Figure S14 (reverse process, cis-to-trans isomer formation). Although relatively slow, the quenched fluorescence of the PDI-dimer was recovered to some extent in the reversible trans-isomer formation (Figure S14b). These results confirm photostability of the PDI-dimer during cis-trans and trans-cis reversible processes, a sought out property for these compounds to be useful for any photo-device applications. Expectedly, for the PDI-control 2 having an azobenzene entity, reversible trans→cis→trans isomerization was observed by the respective 355 or 436 nm pulsed laser irradiation, as shown in Figure S15 (Supporting Information). However, changes in fluorescence intensity during the reversible isomerization were within the experimental error ($<10\%$). Quenching observed in photoirradiated PDI-dimer irrespective of the solvent polarity and not in the control compounds is noteworthy here.

It may be pointed here that azobenzene is known to be a weakly fluorescent compound emitting in the 500–900 nm region with quantum yields in the order of 10^{-6} to 10^{-7} (depending on the isomer and solvent).[11] Control experiments were also performed to verify excited state energy transfer from singlet excited azobenzene to PDI, however, no conclusive evidence could be obtained mainly due to very low quantum yield of azobenzene.

Electrochemical studies using differential pulse (DPV) and cyclic voltammetry (CV) were performed, as shown in Figure 2d and Figure S16. For this, first, the DPV of trans PDI-dimer was recorded in benzonitrile containing 0.1 M (TBA)ClO$_4$ as supporting electrolyte. Next, the contents of the electrochemical cell

were subjected to laser irradiation for 120 s where trans→cis/trans isomerization was observed and the voltammogram was recorded immediately. From such studies, trans PDI-dimer's first reduction and first oxidation at −1.016 and 1.098 V versus Fc/Fc$^+$, and cis/trans PDI-dimer's first reduction and first oxidation at −1.004 and 1.104 V versus Fc/Fc$^+$ were noted. Cyclic voltammetry experiments confirmed reversibility of the reduction and quasi- reversibility of the oxidation processes. The relatively small anodic shift of the cis/trans PDI-dimer (<10–15 mV) was within the experimental error. Further, CVs and DPVs of PDI-control 1 and PDI-control 2 were also recorded to make sure that the azobenzene linker is not redox-active within the potential window where PDI-centred redox processes occur. As shown in Figure S16 (Supporting Information), electrochemical behaviour of control PDIs was similar to that of PDI-dimer, indicating electrochemical inactivity of azobenzene linker in the dimer. The electrochemical HOMO-LUMO gaps (potential difference between the first reduction and first oxidation) for the trans and cis/trans PDI-dimer were found to be 2.114 and 2.108 V, that compared with the spectral $E_{0,0}$ gap of 2.27 eV (same for both trans and cis/trans PDI-dimers), that is, the electrochemical gap was smaller by 0.16 V. These results indicate thermodynamic feasibility of ^{1}PDI* to undergo charge transfer/separation in both trans and cis/trans PDI-dimers.

Spectroelectrochemical data during first reduction and first oxidation of PDI-dimer are shown in Supporting Information, Figures S17a–b. During the course of the first reduction ($E_{appl}=$ −0.38 V vs. Ag/AgCl), original peaks of PDI revealed a decrease with the appearance of new peaks at 713, 811, 878 and 868 nm corresponding to PDI$^{•-}$. Two isosbestic points at 450 and 560 nm were observed. Reversing the potential to 0.00 V, resulted in complete recovery of the original PDI spectrum. During oxidation ($E_{appl}=1.51$ V vs. Ag/AgCl), a new peak at 712 nm corresponding to the formation of PDI$^{•+}$ was observed. These results tracked those reported in the literature for PDI spectroelectrochemistry.[1k,3a] The small red-shift observed in the case of PDI$^{•+}$ compared to that reported for pristine PDI$^{•+}$ could be attributed to the presence of azobenzene. Using spectroelectrochemical data, differential spectrum of the charge separation product, PDI$^{•+}$–PDI$^{•-}$ was constructed as shown in Figure S17c (spectrum of the cation plus anion minus neutral compound). Bleached peaks at 498 and 532 nm due to loss of original neutral compound, and positive peaks at 714, 813, 875 and 960 nm corresponding to PDI$^{•+}$–PDI$^{•-}$ were observed. Such spectrum becomes important in the interpretation of the transient data that will be discussed later.

The geometries of the trans and cis isomers of PDI-dimer were computed using DFT calculations at the B3LYP/6-311G (d,p) level.[12] Coordinates of the optimized structures are listed in the Supporting Information. As shown in Figure 3a, in the case of trans PDI-dimer, the azobenzene spacer, having a C_{2h} symmetry, was almost orthogonal to the PDI entities of the dimer (dihedral angle$=77.8°$). The two PDI entities were almost in the same plane with an edge-to-edge distance of 13.6 Å. In contrast, in the case of the cis PDI-dimer, the azobenzene spacer had roughly a C_2 geometry similar to that shown in Figure 1a (see Figure 3b). The PDI entities, that were in the
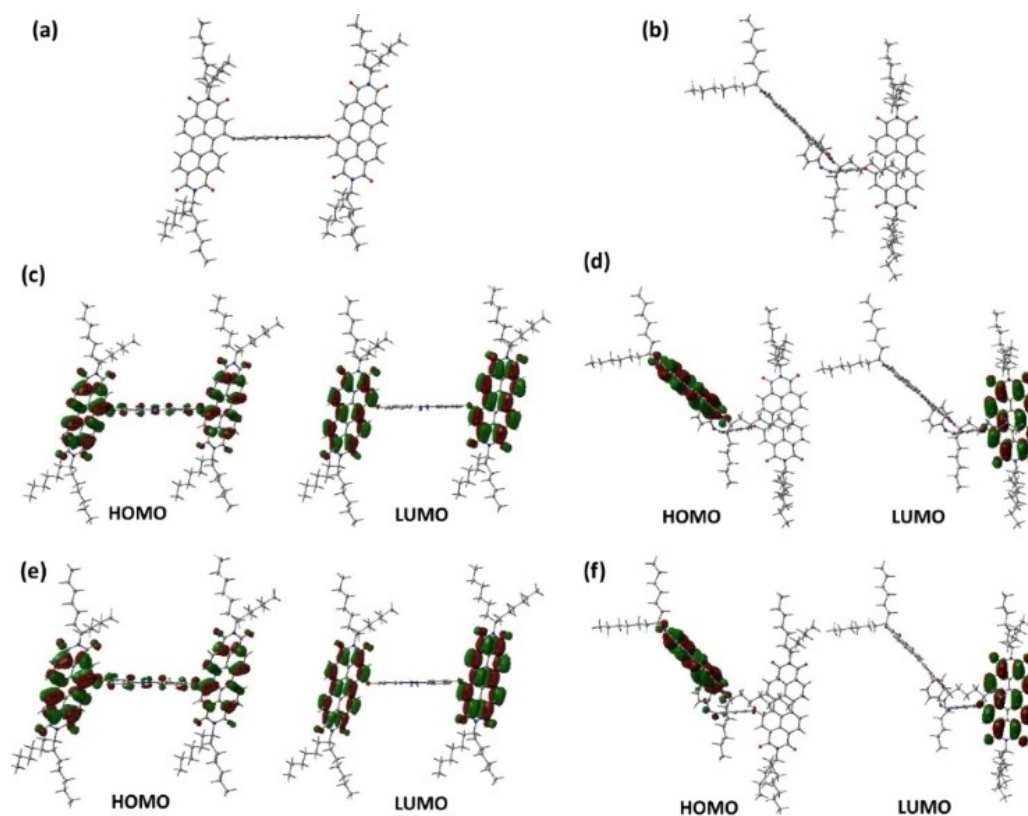
Chemistry–A European Journal

Full Paper
doi.org/10.1002/chem.202102903

Chemistry Europe
European Chemical
Societies Publishing

Figure 3. Optimized structures of (a) trans and (b) cis isomers of PDI-dimer. The frontier HOMO and LUMO in toluene (c and d) and benzonitrile (e and f) are shown.

same plane in the case of trans PDI-dimer, were almost orthogonal in the cis PDI-dimer with a dihedral angle of 70.5°, and an edge-to-edge distance between the two PDI entities of 6.9 Å.

Next, frontier orbitals were generated for both trans and cis PDI-dimers to seek evidence of charge transfer and separation. If such events occur, one would expect uneven distribution of HOMO and LUMO among the two identical PDI entities and such property would be more pronounced with an increase in the solvent polarity. Two solvents, viz., nonpolar toluene ($\varepsilon =$ 2.38) and polar benzonitrile ($\varepsilon = 26.0$) were thus employed. As shown in Figures 3c–d, unequal distribution of both HOMO and LUMO in toluene for both trans and cis PDI-dimers was observed suggesting charge transfer could be a possibility even in a nonpolar solvent. Moving to the more polar benzonitrile, such uneven distribution was more apparent (Figures 3e–f). It is also important to note that the HOMO of both trans and cis PDI-dimer had a small ($<5\%$) contribution on the azobenzene bridge. This was also the situation in the case of PDI-control 2, as shown in Figure S18 (Supporting Information). Although no redox activity of azobenzene within the employed potential window was observed for both dimer and control compounds, the small amount of electron density located on the azoben-zene entity is suggestive of its involvement, perhaps to a lesser extent, in the anticipated charge transfer events. From these observations, it is safe to conclude that the main role of

azobenzene entity is to control the relative orientation of the PDI entities of the dimer and the distance between them, modulating the charge transfer and separation properties, and to a lesser extent to be involved in the anticipated charge transfer events.

To help understand the charge transfer and separation processes as a function of solvent polarity, an energy level diagram was constructed, as shown in Figure 4. Energy of the charge separated states was calculated from Rehm-Weller approach,[13] using the earlier discussed spectral, computational and electrochemical data; the details of these calculations and the data are given in Supporting Information. From fluorescence lifetime quenching and location of frontier orbitals, in both nonpolar and polar solvents, thermodynamically feasible charge transfer resulting into the formation of PDI$^{\delta+}$–PDI$^{\delta-}$ from the singlet excited PDI (^{1}PDI*) could be envisioned. The next step depends on solvent polarity. Polar benzonitrile and DMF solvents, due to solvent stabilization of radical-ion pairs, could promote charge separation resulting in the formation of PDI$^{\bullet+}$–PDI$^{\bullet-}$ (marked in red). It is also important to note that the relative orientation of PDI entities of the dimer and the presence of oxygen connecting the two PDI rings could disrupt the charge separation process. Further, the charge separation product could relax directly to the ground state as the energy difference between the charge separated state and
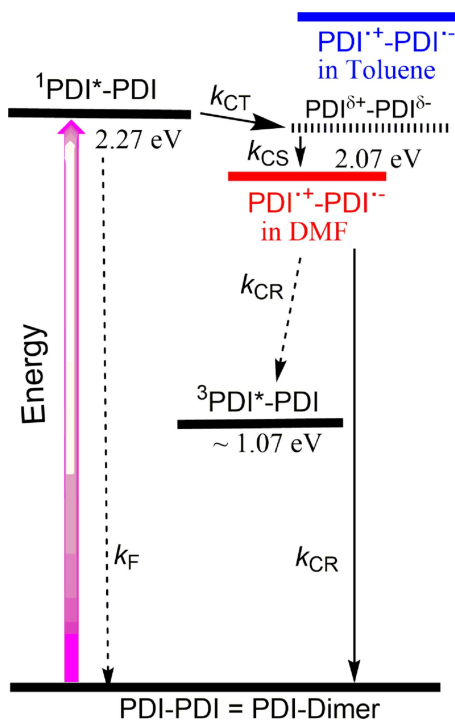
Chem. Eur. J. **2021**, *27*, 14996–15005   www.chemeurj.org

15000   © 2021 The Authors. Chemistry - A European Journal published by Wiley-VCH GmbH

Chemistry–A European Journal

Full Paper
doi.org/10.1002/chem.202102903

**Chemistry
Europe**
European Chemical
Societies Publishing

Figure 4. Energy diagram showing charge transfer and charge separation processes in the PDI-dimer upon photoexcitation. Solid arrow – most likely process. Dashed arrow – less likely process.

the low-lying ^{3}PDI* state is ~1.0 eV making such a process less competitive.[14]

However, in nonpolar toluene, the charge separation process is not favorable as the energy of PDI$^{\bullet+}$–PDI$^{\bullet-}$ state is above that of ^{1}PDI* by ~0.46 eV for the trans isomer and ~0.30 eV for the cis isomer. Under such conditions, the charge transfer state could relax directly to the ground state.

Finally, to experimentally verify the charge transfer and separation processes in the PDI dimer, differential femtosecond transient absorption (fs-TA) spectral studies were systematically performed in solvents of different polarity, as shown in Figure 5 and Figure S19. Figure 5a shows fs-TA of PDI-control 1 in benzonitrile while spectral data for this compound in toluene and DMF are given in Figures S19a and d (Supporting Information). In benzonitrile, immediately after excitation, the instantaneously formed ^{1}PDI* in the PDI-control 1 revealed excited state absorption (ESA) peaks at 692 and 890 nm. Ground state bleach (GSB) and stimulated emission (SE) peaks were located in the 575–625 nm range that had also contribution from scatted excitation light set at 535 nm. With time, the 692 nm peak revealed a red-shift and appeared at 713 nm while the 890 nm peak revealed diminished intensity. However, at the end of 3 ns, the maximum delay time of our instrument, significant amounts of transient spectral features persisted in agreement with the relatively long-lived singlet ^{1}PDI*-control 1 (4.5 to 4.9 ns, see Supporting Information Table S1 for fluorescence decay profiles). Similar spectral trends were observed in toluene and DMF (Figures S19a and d, Supporting Information).

Although known to be inefficient for the earlier mentioned reasons, the ^{1}PDI* could populate the ^{3}PDI* ($E_T = 1.07$ eV)[9] via an intersystem crossing process, hence, efforts were also made to spectrally characterize ^{3}PDI*-control 1 using nanosecond transient absorption (ns-TA) spectroscopy. Direct excitation of PDI-control 1 gave no measurable signal, hence, ^{3}PDI* was populated via energy transfer using anthracene,[13] as shown in Figure S20 (Supporting Information). Main peaks of ^{3}PDI*-control 1 spanned the 550–670 nm range. However, due to strong bleach in the 575–625 nm range and its slow growth, it was difficult to locate the formation of ^{3}PDI* in the control compound.

Fs-TA spectra of the trans and cis/trans PDI-dimers (the latter obtained immediately after 355 nm laser pulse irradiation for 10 min) in benzonitrile are shown in Figures 5b–c while such data in toluene and DMF are shown in Figures S19b,c and e,f, respectively. In both PDI-dimers, the amplitude of the GSB was higher than that of control-2, and the ^{1}PDI* signals revealed faster decay of the ESA peaks and recovery of the GSB/SE peaks. Importantly, with the decay of the ESA peak, new signals overlapped with the ESA signal were observed. Transient features of PDI-control 2, both trans and cis forms, are shown in Figure S21. Here too, faster decay of the ^{1}PDI* was obvious.

Figures 5d–f show the decay profiles of the singlet excited state of PDI-control 1, trans PDI-dimer and cis/trans PDI-dimer in the investigated solvents while decay profiles of PDI-control 2 are shown in Figure S21 (Supporting Information). Two features are clear from visual inspection of these curves, viz., (i) rapid decay of the ^{1}PDI* in the PDI-dimer and PDI-control 2 compared to the PDI-control 1, and (ii) further acceleration of such decay in the cis/trans PDI-dimer. It is worth noting here that although the photo-irradiated dimer was an approximately 1:1 mixture of trans and cis-isomers, its effect is obvious in the measured photophysical properties.

Further careful analysis of the fs-TA data was warranted to confirm occurrence of the charge transfer and separation processes in the dimers. Transient spectra of the controls, and the trans and cis-trans PDI-dimers at a delay time of 500 ps, in the investigated solvents, are shown in Figure 6. Such spectra at earlier delay times (50 ps in toluene, 75 ps in benzonitrile and 100 ps in DMF) are shown in Figure S22 in Supporting Information. The spectrum of the charge-separated state deduced from spectroelectrochemical studies is also shown at the bottom of each panel in Figure 6 and Figure S22. New transient signals at 714, 813, 875 and 960 nm are expected for the PDI$^{\bullet+}$-PDI$^{\bullet-}$ charge-separated state. As shown in Figure 6a-(i), in the case of PDI-control 1 in toluene, ESA peaks of ^{1}PDI* were located at 462, 692, and 858 nm. In the case of PDI-control 2, the last two peaks were found to be red-shifted and appeared at 696 and 865 nm. Such a trend was also observed for the trans and cis/trans dimers in toluene. In addition, there was a peak at 636 nm for the latter compounds. Importantly, no new peaks in the near-IR region expected for PDI$^{\bullet+}$–PDI$^{\bullet-}$ were observed suggesting that no charge separation in PDI-control 2 (with azobenzene entity) and PDI-dimer occurs in toluene. As predicted from Figure 4 and the strong fluorescence quenching, the red-shifted ESA peaks in the PDI-control 2 and PDI-dimer
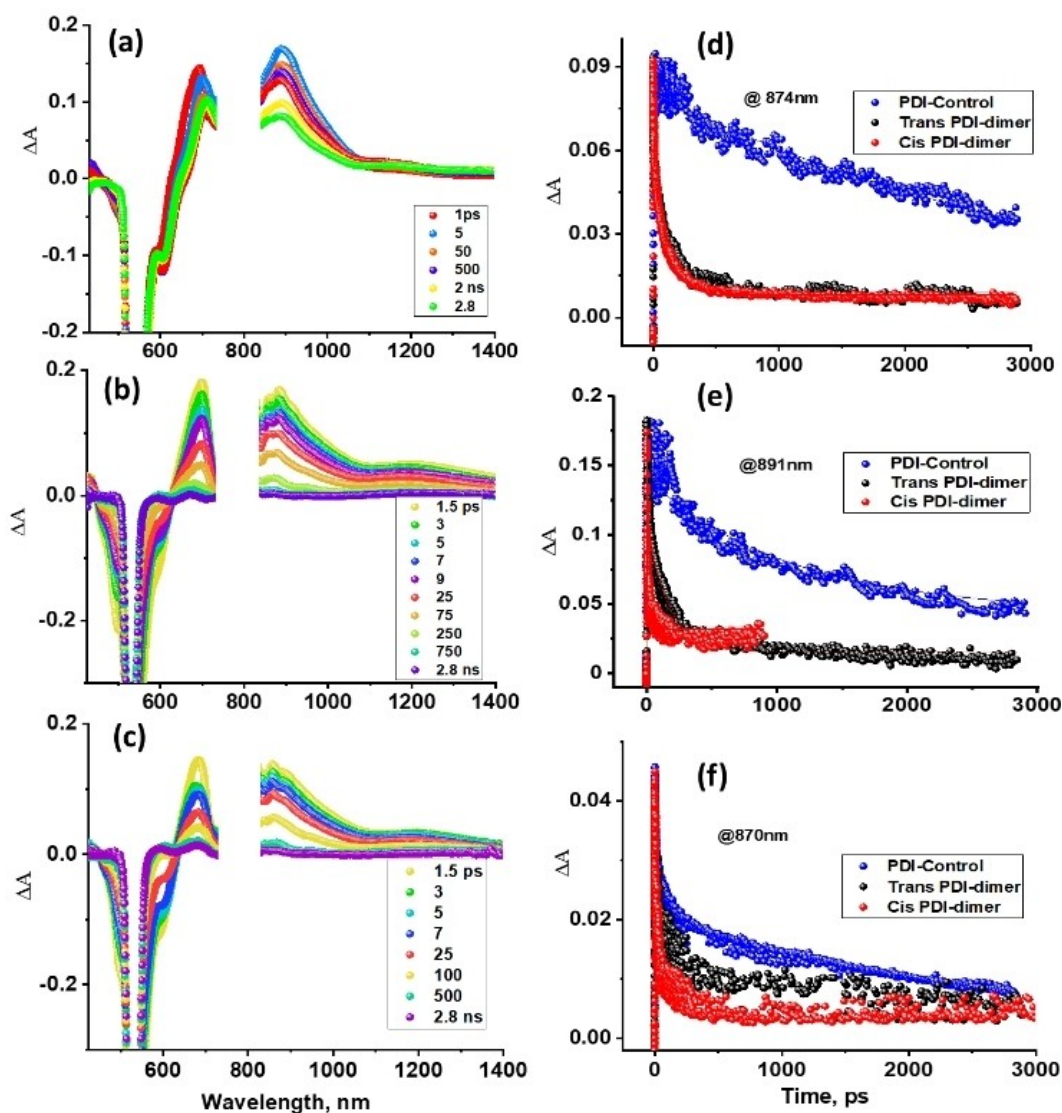
Chemistry–A European Journal

Full Paper
doi.org/10.1002/chem.202102903

Chemistry
Europe
European Chemical
Societies Publishing

Figure 5. Differential femtosecond transient absorption spectra at the indicated delay times of (a) PDI-control 1, (b) trans PDI-dimer and (c) cis/trans PDI-dimer in benzonitrile. The samples were excited at 535 nm corresponding to ^{1}PDI*. The break in 800 nm is due to detector change from visible to near-IR region. Singlet excited state time profiles of PDI-control 1, trans PDI-dimer and cis/trans PDI-dimer in (d) toluene, (e) benzonitrile and (f) DMF.

have been attributed to charge transfer state, $PDI^{\delta+}$–$PDI^{\delta-}$ or $(PDI\text{-}azo)^{\delta+}$–$PDI^{\delta-}$ (azo = azobenzene).

Contrary to these observations, spectral results observed in benzonitrile and DMF were supportive of charge separation in the PDI dimer. As shown in Figures 6b–c, all of the major peaks expected for the charge separated product were clearly observed in polar solvents, more so in DMF (see vertically drawn lines to show position of the peaks, see also Figures S22b–c for growth of these signals at short delay times). In the case of benzonitrile, some contributions from the CT state were obvious even at 500 ps, however, not in more polar DMF. Interestingly, no peak supporting the charge separated state was observed in the case of PDI-control 2 even though it had the azobenzene moiety. These results conclusively prove (i) charge separation involving both PDI entities in PDI-dimer, and (ii) $PDI^{\bullet+}$-$PDI^{\bullet-}$ is the charge-separated species with some

contributions from the azobenzene spacer. That is, symmetry breaking charge separation (SBCS) to a large extent was possible to witness in the present PDI dimer.

Further, the transient data of the PDI-dimer were subjected to Glotaran target analysis[14] to generate species associated spectra (SAS) of different transient species. For both trans and cis-trans PDI-dimer's transient data, at least three components were needed for satisfactory data fit in polar solvents. The SAS and population time profiles in DMF are shown in Figure 7 for the near-IR data. The first component, with few tens to hundred fs time constant, was within the time resolution of our instrument and could be attributed to locally excited S_1* state with contributions from vibrational hot states. The SAS of the second component, with time constants of 16.3 ps for the trans and 13.3 ps for the cis/trans PDI-dimer, was attributed to the charge transfer state. The third component, with time constants of
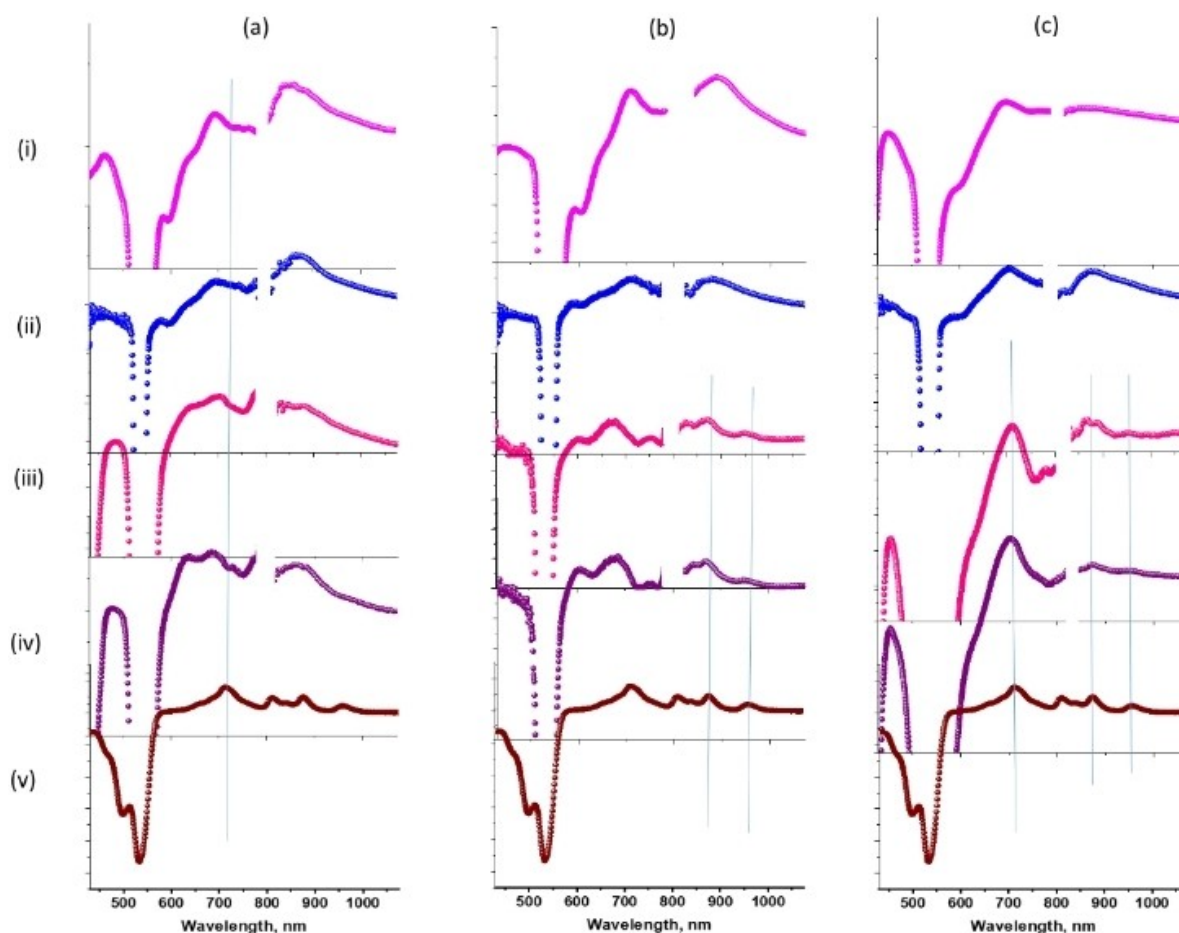
Chemistry–A European Journal

Full Paper
doi.org/10.1002/chem.202102903

Chemistry Europe
European Chemical
Societies Publishing

Figure 6. Fs-TA spectra at a delay time of 500 ps of (i) PDI-control 1, (ii) PDI-control 2, (iii) trans PDI-dimer, (iv) cis/trans PDI-dimer in (a) toluene, (b) benzonitrile, and (c) DMF. The bottom spectra show spectra deduced for charge separated state from spectroelectrochemical studies in benzonitrile. The break in the 800 nm region is due to visible to near-IR detector change.
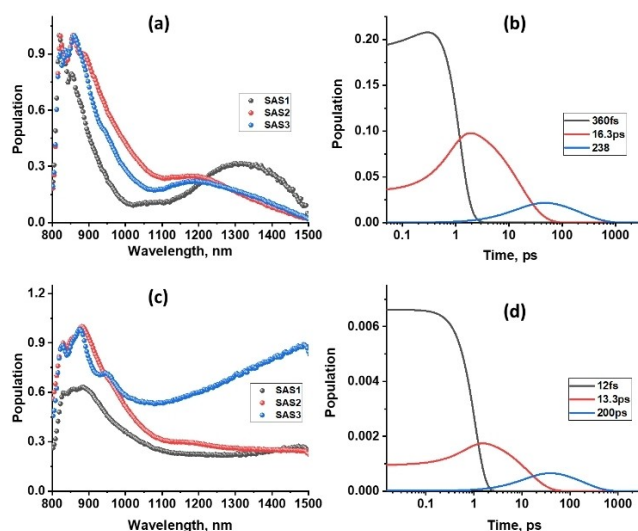

Figure 7. Species associated spectra (SAS) and population time profiles for trans and cis/trans PDI-dimers in DMF (for the fs-TA data shown in Figure 5).

217 ps for the trans and 200 ps for the cis/trans PDI-dimer, and whose SAS had spectral features of the charge-separated state deduced from spectroelectrochemical data in this spectral range, thus was attributed to the charge-separated state. The charge transfer and charge-separated state time constants in PhCN were found to be 20 and 270 ps for the trans PDI-dimer and 16 and 238 ps for the cis/trans PDI-dimer. That is, increasing polarity decreased the average lifetime of both charge transfer and charge-separated states, and such events were even short-lived in the case of cis/trans PDI-dimer. That is, accelerated charge separation in the case of cis/trans PDI-dimer over the trans dimer is witnessed. This has been rationalized to the geometry factor, that is, closer distance between the PDI entities in the cis/trans PDI-dimer compared to that of the trans PDI-dimer (6.7 Å closer for cis-isomer). It may be mentioned here that the values obtained for the cis/trans dimer are the average values as photo-isomerization resulted in a 1:1 mixture of cis and trans isomers. This observation also suggests that if a pure cis-isomer could be obtained by some mechanism it could reveal a much faster charge separation process than the trans one.

Chemistry–A European Journal

Full Paper
doi.org/10.1002/chem.202102903

Chemistry Europe
European Chemical
Societies Publishing

Conclusions

In summary, occurrence of charge transfer and charge separation events upon photo-excitation of a newly synthesized azobenzene bridged PDI dimer, as a function of solvent polarity, has been successfully demonstrated. Additionally, it has been possible to expose the effect of trans to cis/trans isomerization of azobenzene spacer in the PDI dimer in governing the photophysical events. Reversible trans to cis/trans formation was witnessed by irradiation of the PDI-dimer by 355 nm pulsed laser light and by 435 nm light for reversing the process. Substantial fluorescence quenching in the PDI-dimer was observed as compared to monomeric PDI-controls, and such quenching increased with increasing solvent polarity with appreciable red-shifts. Importantly, between the trans and cis/trans dimers, quenching in the latter (containing both isomers) was relatively higher. Frontier orbitals generated from DFT calculations helped in visualizing the charge transfer and separation phenomenon in the PDI-dimer in both isomeric forms, and some participation of the azobenzene linker in the overall charge transfer process. Fs-TA studies confirmed sequential occurrence of ^{1}PDI*-PDI→PDI$^{\delta+}$–PDI$^{\delta-}$→PDI$^{\bullet+}$–PDI$^{\bullet-}$ in both PDI-dimers (trans and cis/trans) in polar solvents. The evaluated time constants from data analysis using Glotaran target analysis revealed accelerated charge separation process in the cis/trans PDI-dimer as compared to its trans analog.

Experimental Section

4,4'-bis[N,N'-di(hexylheptyl)perylene-3'',4'':9'',10''-tetracarboxidiimide-1''-yloxy]azobenzene (PDI Dimer): 4,4'-dihydroxyazobenzene[8] (22 mg, 0.1 mmol), 18-crown-6 (1.06 g, 4 mmol) and CsF (152 mg, 1 mmol) were added to a solution of N,N'-di(hexylheptyl)-1-bromo-3,4:9,10-perylenetetracarboxydiimide,[7] Br-PDI, (208 mg, 0.25 mmol) in dry THF (3 mL). The reaction was refluxed 24 h under argon atmosphere and, after cooling, it was extracted with dichloromethane and washed with water. The organic layer was dried over anhydrous sodium sulfate, filtered and evaporated. Purification was carried out by silica gel column chromatography using dichloromethane:hexane 1:1 as eluent to give compound PDI-Dimer as a red powder (79 mg, 46%). ^{1}H NMR (300 MHz, C$_2$D$_2$Cl$_4$, 70°C): δ 9.52 (d, J=8.3 Hz, 2H), 8.72 (m, 10H), 8.40 (s, 2H), 8.09 (d, J=8.9 Hz, 4H), 7.36 (d, J=8.9 Hz, 4H), 5.18 (m, 4H), 2.24 (m, 8H), 1.94 (m, 8H), 1.30 (m, 64H), 0.89 (t, 24H). ^{13}C NMR (75 MHz, C$_2$D$_2$Cl$_4$, 70°C): δ 164.66, 163.53, 157.19, 155.05, 149.67, 134.52, 133.35, 129.25, 128.66, 126.96, 126.30, 125.50, 124.34, 123.89, 122.77, 119.70, 54.77, 32.41, 31.85, 31.83, 29.33, 29.29, 27.04, 22.73, 22.72, 14.26. EM MALDI-TOF: m/z calcd for C$_{112}$H$_{130}$N$_6$O$_{10}$ [M+H]$^+$ 1719.9921, found 1719.9691. IR (KBr): ν 2966, 2925, 2852, 1699, 1659, 1589, 1491, 1409, 1332, 1266, 1103, 1017, 805 cm^{-1}. UV-vis (CH$_2$Cl$_2$): λmax/nm (log ε): 492 (4.7), 526 (4.9).

N,N'-di(hexylheptyl)-1-phenoxy-3,4:9,10-perylenetetracarboxydiimide (PDI-control 1): Phenol (90 mg, 0.96 mmol), 18-crown-6 (1.26 g, 4.8 mmol) and CsF (182 mg, 1.2 mmol) were added to a solution of N,N'-di(hexylheptyl)-1-bromo-3,4:9,10-perylenetetracarboxydiimide, Br-PDI, (200 mg, 0.24 mmol) in dry THF (3 mL). The reaction was refluxed 24 h under argon atmosphere and, after cooling, it was extracted with dichloromethane and washed with water. The organic layer was dried over anhydrous sodium sulfate, filtered and evaporated. Purification was carried out by silica gel column chromatography using toluene as eluent to give PDI-control 1 as a red powder (170 mg, 84%). ^{1}H NMR (300 MHz, CDCl$_3$) δ 9.53 (d, J=8.4 Hz, 1H), 8.65 (m, 5H), 8.26 (s, 1H), 7.48 (t, J=7.9 Hz, 2H), 7.30 (t, 1H), 7.19 (d, J=8.2 Hz, 2H), 5.18 (m, 2H), 2.22 (m, 4H), 1.84 (m, 4H), 1.22 (m, 32H), 0.82 (t, 12H). ^{13}C NMR (75 MHz, CDCl$_3$) δ 167.57, 166.59, 159.13, 157.78, 137.35, 136.70, 133.79, 132.22, 131.58, 131.52, 129.95, 128.82, 128.53, 126.75, 126.48, 125.53, 122.89, 57.73, 35.41, 34.85, 34.82, 32.34, 32.28, 30.05, 25.73, 25.71, 17.26, 17.25. EM MALDI-TOF: m/z calcd for C$_{56}$H$_{66}$N$_2$O$_5$ [M$^+$] 846.4966, found 846.4177. IR (KBr): ν 2956, 2921, 2845, 1713, 1660, 1596, 1415, 1334, 1264, 814, 738 cm^{-1}. UV-vis (CH$_2$Cl$_2$): λmax/nm (log ε): 495 (4.6), 528 (4.7).

N,N'-di(hexylheptyl)-1-(4'-phenylazophenoxy)-3,4:9,10-perylene tetracarboxydiimide (PDI-control 2): 4-phenylazophenol (190 mg, 0.96 mmol), 18-crown-6 (1.26 g, 4.8 mmol) and CsF (182 mg, 1.2 mmol) were added to a solution of N,N'-di(hexylheptyl)-1-bromo-3,4:9,10-perylenetetracarboxydiimide, Br-PDI, (200 mg, 0.24 mmol) in dry THF (3 mL). The reaction was refluxed 24 h under argon atmosphere and, after cooling, it was extracted with dichloromethane and washed with water. The organic layer was dried over anhydrous sodium sulfate, filtered and evaporated. Purification was carried out by silica gel column chromatography using dichloromethane:hexane (3:1) as eluent to give PDI-control 2 as a red powder (110 mg, 48%). ^{1}H NMR (300 MHz, CDCl$_3$) δ 9.49 (d, J=8.4 Hz, 1H), 8.68 (m, 5H), 8.32 (br, 1H), 8.03 (d, J=8.8 Hz, 2H), 7.90 (d, J=8.2 Hz, 2H), 7.50 (m, 3H), 7.31 (d, J=8.8 Hz, 2H), 5.17 (m, 2H), 2.21 (m, 4H), 1.86 (m, 4H), 1.22 (m, 32H), 0.81 (t, 12H). ^{13}C NMR (75 MHz, CDCl$_3$) δ 164.34, 163.47, 162.68, 156.93, 154.96, 152.46, 149.60, 134.29, 134.11, 133.16, 130.98, 129.14, 128.99, 128.49, 128.40, 126.80, 126.16, 125.22, 123.48, 122.76, 122.36, 120.18, 119.49, 54.60, 32.26, 31.65, 31.63, 29.59, 29.11, 29.08, 26.82, 22.46, 14.00, 13.91. EM MALDI-TOF: m/z calcd for C$_{62}$H$_{70}$N$_4$O$_5$ [M–H]$^+$ 949.5340, found 949.5778. IR (KBr): ν 2961, 2921, 2856, 1695, 1649, 1596, 1409, 1339, 1258, 1024, 820 cm^{-1}. UV-vis (CH$_2$Cl$_2$): λmax/nm (log ε): 492 (4.6), 525 (4.8).

Conflict of Interest

The authors declare no conflict of interest.

[1] a) B. Dereka, A. Rosspeintner, M. Krzeszewski, D. T. Gryko, E. Vauthey, *Angew. Chem. Int. Ed.* **2016**, *55*, 15624–15628; *Angew. Chem.* **2016**, *128*,

15853–15857; b) V. Markovic, D. Villamaina, I. Barabanov, L. M. Lawson Daku, E. Vauthey, *Angew. Chem. Int. Ed.* **2011**, *50*, 7596–7598; *Angew. Chem.* **2011**, *123*, 7738–7740; c) A. Aster, G. Licari, F. Zinna, E. Brun, T. Kumpulainen, E. Tajkhorshid, J. Lacour, E. Vauthey, *Chem. Sci.* **2019**, *10*, 10629–10639; d) E. Vauthey, *ChemPhysChem* **2012**, *13*, 2001–2011; e) J. M. Giaimo, A. V. Gusev, M. R. Wasielewski, *J. Am. Chem. Soc.* **2002**, *124*, 8530–8531; f) R. M. Young, M. R. Wasielewski, *Acc. Chem. Res.* **2020**, *53*, 1957–1968; g) C. E. Ramirez, S. Chen, N. E. Powers-Riggs, I. Schlesinger, R. M. Young, M. R. Wasielewski, *J. Am. Chem. Soc.* **2020**, *142*, 18243–18250; h) K. Miyata, Y. Kurashige, K. Watanabe, T. Sugimoto, S. Takahashi, S. Tanaka, J. Takeya, T. Yanai, Y. Matsumoto, *Nat. Chem.* **2017**, *9*, 983; i) T. Kim, J. Kim, H. Mori, S. Park, M. Lim, A. Osuka, D. Kim, *Phys. Chem. Chem. Phys.* **2017**, *19*, 13970–13977; j) B. Carlotti, E. Benassi, A. Spalletti, C. G. Fortuna, F. Elisei, V. Barone, *Phys. Chem. Chem. Phys.* **2014**, *16*, 13984–13994; k) J. Kong, W. Zhang, G. Li, D. Huo, Y. Guo, X. Niu, Y. Wan, B. Tang, A. Xia, *J. Phys. Chem. Lett.* **2020**, *11*, 10329–10339; l) M. T. Whited, N. M. Patel, S. T. Roberts, K. Allen, P. I. Djurovich, S. E. Bradforth, M. E. Thompson, *Chem. Commun.* **2012**, *48*, 284–286; m) J. H. Golden, L. Estergreen, T. Porter, A. C. Tadle, D. Sylvinson M R, J. W. Facendola, C. P. Kubiak, S. E. Bradforth, M. E. Thompson, *ACS Appl. Energ. Mater.* **2018**, *1*, 1083–1095; n) M. Kellogg, A. Akil, D. S. M. Ravinson, L. Estergreen, S. E. Bradforth, M. E. Thompson, *Faraday Discuss.* **2019**, *216*, 379–394.

[2] T. Arlt, S. Schmidt, W. Kaiser, C. Lauterwasser, M. Meyer, H. Scheer, W. Zinth, *Proc. Nat. Acad. Sci.* **1993**, *90*, 11757–11761.

[3] a) Y. Wu, R. M. Young, M. Frasconi, S. T. Schneebeli, P. Spenst, D. M. Gardner, K. E. Brown, F. Würthner, J. F. Stoddart, M. R. Wasielewski, *J. Am. Chem. Soc.* **2015**, *137*, 13236–13239; b) H. Liu, V. M. Nichols, L. Shen, S. Jahansouz, Y. Chen, K. M. Hanson, C. J. Bardeen, X. Li, *Phys. Chem. Chem. Phys.* **2015**, *17*, 6523–6531; c) E. A. Margulies, L. E. Shoer, S. W. Eaton, M. R. Wasielewski, *Phys. Chem. Chem. Phys.* **2014**, *16*, 23735–23742; d) N. Saki, T. Dinc, E. U. Akkaya, *Tetrahedron* **2006**, *62*, 2721–2725.

[4] a) G. S. Hartley, *Nature* **1937**, *140*, 281; b) T. Schultz, J. Quenneville, B. Levine, A. Toniolo, T. J. Martínez, S. Lochbrunner, M. Schmitt, J. P. Shaffer, M. Z. Zgierski, A. Stolow, *J. Am. Chem. Soc.* **2003**, *125*, 8098–8099; c) H. D. Bandara, S. C. Burdette, *Chem. Soc. Rev.* **2012**, *41*, 1809–1825.

[5] a) W. Ling, X. Cheng, T. Miao, S. Zhang, W. Zhang, X. Zhu, *Polymer* **2019**, *11*, 1143; b) K. Y. Chiu, Y.-J. Tu, C.-J. Lee, T.-F. Yang, L.-L. Lai, I. Chao, Y. O. Su, *Electrochim. Acta* **2012**, *62*, 51–62; c) J. L. Rodríguez-Redondo, Á.

Sastre-Santos, F. Fernández-Lázaro, D. Soares, G. C. Azzellini, B. Elliott, L. Echegoyen, *Chem. Commun.* **2006**, 1265–1267.

[6] N. Zink-Lorre, E. Font-Sanchis, Á. Sastre-Santos, F. Fernández-Lázaro, *Org. Chem. Front.* **2017**, *4*, 2016–2021.

[7] Q. Yan, D. Zhao, *Org. Lett.* **2009**, *11*, 3426–3429.

[8] J. Wang, Q. Jiang, X. Hao, H. Yan, H. Peng, B. Xiong, Y. Liao, X. Xie, *RSC Adv.* **2020**, *10*, 3726–3733.

[9] L. Martín Gomis, R. Díaz-Puertas, S. Seetharaman, P. A. Karr, F. Fernández-Lázaro, F. D'Souza, Á. Sastre-Santos, *Chem. Eur. J.* **2020**, *26*, 4822–4832.

[10] J. R. Lakowicz in *Principles of Fluorescence Spectroscopy*, Springer Science & Business Media, **2013**.

[11] H. Satzger, S. Sporlein, C. Root, J. Wachtveitl, W. Zinth, P. Gllch, *Chem. Phys. Lett.* **2003**, *372*, 216–223.

[12] *Gaussian 16*, Revision A.03, M. J. Frisch, G. W. Trucks, H. B. Schlegel, G. E. Scuseria, M. A. Robb, J. R. Cheeseman, G. Scalmani, V. Barone, B. Mennucci, G. A. Petersson, H. Nakatsuji, M. Caricato, X. Li, H. P. Hratchian, A. F. Izmaylov, J. Bloino, G. Zheng, J. L. Sonnenberg, M. Hada, M. Ehara, K. Toyota, R. Fukuda, J. Hasegawa, M. Ishida, T. Nakajima, Y. Honda, O. Kitao, H. Nakai, T. Vreven, J. A. Montgomery Jr., J. E. Peralta, F. Ogliaro, M. Bearpark, J. J. Heyd, E. Brothers, K. N. Kudin, V. N. Staroverov, R. Kobayashi, J. Normand, K. Raghavachari, A. Rendell, J. C. Burant, S. S. Iyengar, J. Tomasi, M. Cossi, N. Rega, J. M. Millam, M. Klene, J. E. Knox, J. B. Cross, V. Bakken, C. Adamo, J. Jaramillo, R. Gomperts, R. E. Stratmann, O. Yazyev, A. J. Austin, R. Cammi, C. Pomelli, J. W. Ochterski, R. L. Martin, K. Morokuma, V. G. Zakrzewski, G. A. Voth, P. Salvador, J. J. Dannenberg, S. Dapprich, A. D. Daniels, Ö. Farkas, J. B. Foresman, J. V. Ortiz, J. Cioslowski, D. J. Fox, Gaussian, Inc., Wallingford, CT, USA, USA, **2016**.

[13] D. Rehm, A. Weller, *Isr. J. Chem.* **1970**, *10*, 259–271.

[14] A. Kohler, H. Bassler, *Mater. Sci. Eng. R* **2009**, *66*, 71–109.

[15] a) W. E. Ford, P. V. Kamat, *J. Phys. Chem.* **1987**, *91*, 6373–6380; b) T. Kircher, H.-G. Löhmannsröben, *Phys. Chem. Chem. Phys.* **1999**, *1*, 3987–3992.

[16] a) http://glotaran.org/; b) J. Snellenburg, S. Laptenok, R. Seger, K. Mullen, I. Van Stokkum, *J. Stat. Softw.* **2012**, *49*, 1–22.